

# Neuron Growth Output-Feedback Control by PDE Backstepping

Cenk Demir<sup>1</sup> Shumon Koga<sup>2</sup> and Miroslav Krstic<sup>1</sup>

**Abstract**—Neurological injuries predominantly result in loss of functioning of neurons. These neurons may regain function after particular medical therapeutics, such as Chondroitinase ABC (ChABC), that promote axon elongation by manipulating the extracellular matrix, the network of extracellular macromolecules, and minerals that control the tubulin protein concentration, which is fundamental to axon elongation. We introduce an observer for the concentration of unmeasured tubulin along the axon, as well as in the growth cone, using the measurement of the axon length and the tubulin flux at the growth cone. We employ this observer in a boundary control law which actuates the tubulin concentration at the soma (nucleus), i.e., at the end of the axon distal from the measurement location. For this PDE system with a moving boundary, coupled with a two-state ODE system, we establish global exponential convergence of the observer and local exponential stabilization of the [axon, observer] system in the spatial  $\mathcal{H}_1$ -norm. The results require that the axon growth speed be bounded. For an open-loop observer, this is ensured by assumption (which requires that tubulin influx at the soma be limited), whereas for the output-feedback system the growth rate of the axon is ensured by assuming that the initial conditions of all the states, including the axon length, be sufficiently close to their setpoint values.

## I. INTRODUCTION

Neuroscience is a complex interdisciplinary research field aimed at enhancing understanding of how neurons perceive information and curing nervous system-related disorders and damage [12], [24], [22]. These disorders and impairments, such as Parkinson’s disease, Alzheimer’s disease, Huntington’s disease, and spinal cord injuries, may occur because of the degeneration of neurons [19], [7], [18]. These medical disorders regularly result from the loss of functionality of neurons, such as the cessation of elongation. Treatments such as ChABC can heal neurons and resume their activities [14], [2]. The basic idea of this therapy is to manipulate the extracellular matrix (ECM) to regulate the activity of neurons as desired [11].

Neurons are highly active cells whose mission is to receive and transmit electrical signals which contain perceptual information. This process begins with a signal entry from the dendrites of a postsynaptic neuron. It continues with the transportation of the signal through the axon by using the energy produced in the soma. During transmission, the growth cone, located at the end of the axon, seeks the chemical cues to detect the neuron that will receive the signal [13]. After detecting the direction, tubulin dimers and

monomers assemble to create microtubules which extend the axon with the assistance of ECM [1]. Thus, tubulin concentration dynamics in the axon are the primary regulator of axon elongation. These dynamics express the following behaviors: the tubulin production in the soma, assembly and disassembly processes of microtubules in the axon, and the transportation process along the axon and in the growth cone [9]. Recent preclinical studies show that manipulation of ECM controls the axon growth, by which the tubulin concentration is controlled [4].

Researchers proposed different mathematical models to explain the axon growth process by considering most or some of the behavior of tubulin. One of the pioneer mathematical models describes the polymerization of tubulin [5]. In another model developed in [27], the authors propose tubulin transportation as diffusion and include the axon growth due to the polymerization process. A PDE model of axon growth is presented in [21], and its stability properties are defined in [20]. Another pioneer axon growth model introduces a coupled PDE-ODE with a moving boundary and gives numerical results for tubulin concentration along the axon [10].

Besides computational purposes, the coupled PDE-ODE axon growth model has also begun to be studied from a control-theoretical perspective to stabilize the axon growth [8]. Recent enhancements related to the boundary control of PDEs have motivated researchers in different fields [17]. The contribution of [23] has introduced the method of successive approximation to obtain solutions to kernel PDEs for Volterra type of transformation for parabolic PDEs. These groundbreaking studies have extended the type of systems accompanied with boundary control to the class of coupled PDE-ODE systems [25], [26]. While almost all of the studies dealt with a constant domain size in time, the authors of [15], [16] have developed a backstepping design for a parabolic PDE with a moving boundary, called the Stefan problem. The authors have proven the global exponential stability of the closed-loop system with the proposed input by means of both state-feedback and output-feedback control. In addition, recent research considers nonlinear PDE systems and proves the stability results in a local sense [6], [3]. While those results about local stabilization for nonlinear PDE systems have been achieved for hyperbolic PDEs, an output-feedback stabilization for the coupled nonlinear parabolic PDE-ODE with a moving boundary, which is a class of the system modeling axon growth dynamics proposed in literature, has not been studied so far.

This paper present the output-feedback stabilization for the tubulin concentration model associated with the axon

<sup>1</sup>Cenk Demir and Miroslav Krstic are with the Department of Mechanical and Aerospace Engineering, U.C. San Diego, 9500 Gilman Drive, La Jolla, CA, 92093-0411, cdemir@ucsd.edu and krstic@ucsd.edu

<sup>2</sup>Shumon Koga is with the Department of Electrical and Computer Engineering, U.C. San Diego, 9500 Gilman Drive, La Jolla, CA, 92093-0411, skoga@ucsd.edu

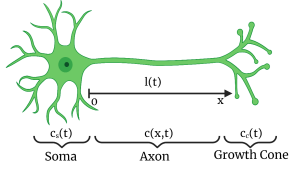


Fig. 1: Schematic of neuron and state variables

growth dynamics, described by a parabolic PDE with moving boundary governed by a nonlinear ODE. First, we obtain the linearized reference error system by considering the error variable from the steady-state solution of the system in the plant dynamics for a given desired axon length, and applying the linearization to ODE state in order to deal with algebraic nonlinearity. By setting the measured output of the system as the axon length and the change of the tubulin concentration in growth cone, we design an observer to estimate the plant state with an observer gain which is given by the kernel functions via the backstepping technique. Since these kernels are not analytically solvable, we apply the method of successive approximation to guarantee the well-posedness of the solution. We rigorously prove the global stability for the observer error system, and the local stability result for the closed-loop system with the output-feedback control following the similar procedure to [8]. The numerical simulation is performed to investigate the performance of the proposed observer and output-feedback control designs, which illustrates the desired performance in both regulation of the axon growth and the estimation of the tubulin concentration.

The paper is structured as follows. Section II introduces the coupled PDE-ODE system with a moving boundary modeling the tubulin concentration and the axon growth. Section III presents the observer design via backstepping method, the method of successive approximation, and the stability analysis of the estimation error system. Section IV proposes the observer-based output-feedback control and the stability proof of closed-loop system. Section V provides the simulation result for the closed-loop system of the axon growth model using the verified physical parameters with the proposed observer and output-feedback control. The paper ends with the conclusion in Section VI.

## II. MODELING OF AXON GROWTH

This section presents the mathematical model of the axon elongation process governed by a coupled PDE-ODE with a moving boundary. In this model, the concentration of tubulin protein along the axon directly controls the growth of a newborn axon. There are two underlying assumptions for modeling the axonal growth given here. The first assumption is that the tubulin protein is entirely responsible for the growth of an axon, not any other substance. The second assumption is that free tubulin molecules are modeled as homogeneous continuums because of their small size.

Let  $l(t)$  denote the length of axon,  $x$  denote the one-dimensional coordinate along the axon, and  $c(x, t)$  denote the

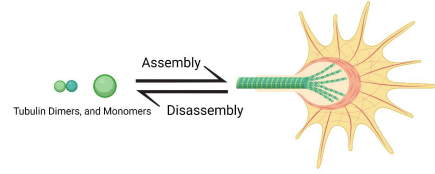


Fig. 2: Tubulin assembly-disassembly

tubulin concentration along this one-dimensional coordinate. The variables with subscripts  $c$ , and  $s$  describe the ones of growth cone and soma, namely,  $c_c(t)$  and  $c_s(t)$  are the tubulin concentration in the growth cone and soma, respectively, as shown in Fig. 1. While free tubulin proteins move with the constant velocity  $a$ , and diffuse with the diffusivity constant  $D$ , the degradation along the axon occurs with the constant rate  $g$ . The constant  $l_c$  is the growth ratio of growth cone,  $\tilde{r}_g$  is the chemical reaction rate of free tubulin monomers and dimers to create microtubules, which is shown in Fig. 2. Taking into account all of these effects, the dynamics of the tubulin concentration associated with the dynamics of the axon length are described as

$$c_t(x, t) = Dc_{xx}(x, t) - ac_x(x, t) - gc(x, t), \quad (1)$$

$$c_x(0, t) = -q_s(t), \quad (2)$$

$$c(l(t), t) = c_c(t), \quad (3)$$

$$l_c \dot{c}_c(t) = (a - gl_c)c_c(t) - Dc_x(l(t), t) - (r_g c_c(t) + \tilde{r}_g l_c)(c_c(t) - c_\infty), \quad (4)$$

$$\dot{l}(t) = r_g(c_c(t) - c_\infty), \quad (5)$$

where  $r_g$  is a lumped parameter introduced in [9], and  $c_\infty$  is a equilibrium concentration in the cone to stop the axonal growth.

Let  $c_{eq}(x)$  be the tubulin concentration profile for a given constant axon length  $l_s$ , the solution of which is given in [10]. Let  $u(x, t)$ ,  $z_1(t)$ ,  $z_2(t)$ , and  $U(t)$  be the reference error states and input defined below:

$$u(x, t) = c(x, t) - c_{eq}(x), \quad (6)$$

$$z_1(t) = c_c(t) - c_\infty, \quad (7)$$

$$z_2(t) = l(t) - l_s, \quad (8)$$

$$U(t) = -(q_s(t) - q_s^*). \quad (9)$$

By subtracting the steady-state solution from (1)-(5), and using (6)-(9), we obtain the reference error system as in [8]. The reference error system has algebraic nonlinearity in ODE of the dynamics, so the linearization technique mentioned above is applied to deal with the nonlinearity. Then, we obtain the following dynamics (see Section 12-2 in [16] for the details):

$$u_t(x, t) = Du_{xx}(x, t) - au_x(x, t) - gu(x, t), \quad (10)$$

$$u_x(0, t) = U(t), \quad (11)$$

$$u(l(t), t) = H^T X(t), \quad (12)$$

$$\dot{X}(t) = AX(t) + Bu_x(l(t), t), \quad (13)$$

where  $X(t) = [z_1(t) \ z_2(t)]^\top$  and

$$A = \begin{bmatrix} \tilde{a} & 0 \\ r_g & 0 \end{bmatrix}, \quad B = \begin{bmatrix} -\beta \\ 0 \end{bmatrix}, \quad (14)$$

$$H = \begin{bmatrix} 1 & -\frac{(a - gl_c)c_\infty}{D} \end{bmatrix}^\top. \quad (15)$$

**Control Design Task:** Develop an observer-based output-feedback control law for the input  $q_s(t)$  so that  $l(t)$  converges to a desired (setpoint) axon length  $l_s > 0$ , at least starting from  $c(x, 0)$  sufficiently near  $c_{\text{eq}}(x)$  (in a suitable norm in  $x$ ) and  $l(0)$  sufficiently near  $l_s$ .

### III. STATE ESTIMATION DESIGN

In this section, first we state the assumptions on the axon length. Then, we propose the first major theorem in this paper with providing its proof, the exponential stability of the observer error system.

**Assumption 1.** *The axon length  $l(t)$  maintains positive and is upper bounded, i.e., there exists a positive constant  $\bar{l} > 0$  such that the following inequality holds:*

$$0 < l(t) \leq \bar{l}, \quad (16)$$

for all  $t \geq 0$ .

**Assumption 2.** *The time derivative of the axon length is also bounded, i.e., there exists a positive constant  $\bar{v} > 0$  such that the following inequality holds:*

$$|\dot{l}(t)| \leq \bar{v}, \quad (17)$$

for all  $t \geq 0$ .

Before we state our major theorem, we define the  $\mathcal{H}_1$ -norm as  $\|f(\cdot, t)\|_{\mathcal{H}_1} = \sqrt{\int_0^{l(t)} f^2(\cdot, t) + f_x^2(\cdot, t) dx}$ .

**Theorem 1.** *Let Assumptions 1 and 2 hold. Consider the plant (10)-(13) and the available measurements*

$$y_1(t) = u_x(l(t), t), \quad y_2(t) = CX(t) \quad (18)$$

where  $C = [0 \ 1]$ . Also, consider the observer designed as

$$\begin{aligned} \hat{u}_t(x, t) &= D\hat{u}_{xx}(x, t) - a\hat{u}_x(x, t) - g\hat{u}(x, t) \\ &\quad + p_1(x, l(t)) (u_x(l(t), t) - \hat{u}_x(l(t), t)), \end{aligned} \quad (19)$$

$$\hat{u}_x(0, t) = U(t), \quad (20)$$

$$\hat{u}(l(t), t) = H^T \hat{X}(t), \quad (21)$$

$$\begin{aligned} \dot{\hat{X}}(t) &= A\hat{X}(t) + Bu_x(l(t), t) + LC(X(t) - \hat{X}(t)), \\ &\quad (22) \end{aligned}$$

where  $x \in [0, l(t)]$ ,  $L$  is chosen to make  $A - LC$  Hurwitz, and the observer gain  $p_1(x, l(t)) = DP(x, l(t))$  where  $P(x, l(t))$  is the solution to the following PDE

$$\begin{aligned} DP_{yy}(x, y) - DP_{xx}(x, y) + aP_x(x, y) \\ - aP_y(x, y) = \lambda P(x, y), \end{aligned} \quad (23)$$

$$P(x, x) = \left( \frac{\lambda}{2D}x + \gamma_1 \right), \quad (24)$$

$$P_x(0, y) = 0, \quad (25)$$

where  $\lambda > 0$  is an arbitrary constant, and  $\gamma_1$  is a constant satisfying  $\frac{D}{a} \leq \gamma_1$ . Then, the observer error system is exponentially stable in  $\mathcal{H}_1$ -norm, i.e., there exist positive constants  $M > 0$  and  $\kappa > 0$  such that the following norm estimate holds:

$$\tilde{\Phi}(t) \leq M\tilde{\Phi}(0)e^{-\kappa t}, \quad (26)$$

where  $\tilde{\Phi}(t) := \|u - \hat{u}\|_{\mathcal{H}_1} + |X - \hat{X}|$ .

Theorem 1 is proved in the remainder of this section.

#### A. Observer design and backstepping transformation

1) *Observer design and observer error system:* Then, we define the observer error state as

$$\tilde{u}(x, t) = u(x, t) - \hat{u}(x, t), \quad \tilde{X}(t) = X(t) - \hat{X}(t). \quad (27)$$

Subtracting the observer system (19)-(22) from the plant (10)-(13), the observer error dynamics is obtained as

$$\begin{aligned} \tilde{u}_t(x, t) &= D\tilde{u}_{xx}(x, t) - a\tilde{u}_x(x, t) - g\tilde{u}(x, t) \\ &\quad + p_1(x, l(t))\tilde{u}_x(l(t), t), \end{aligned} \quad (28)$$

$$\tilde{u}_x(0, t) = 0, \quad (29)$$

$$\tilde{u}(l(t), t) = H^T \tilde{X}(t), \quad (30)$$

$$\dot{\tilde{X}}(t) = (A - LC) \tilde{X}(t). \quad (31)$$

2) *Inverse backstepping transformation:* We consider the backstepping transformation in the inverse form as

$$\tilde{u}(x, t) = \tilde{w}(x, t) + \int_x^{l(t)} P(x, y)\tilde{w}(y, t)dy, \quad (32)$$

where  $P(x, y) \in \mathbb{R}$  is the gain kernel to be solved. Let the target system be

$$\begin{aligned} \tilde{w}_t(x, t) &= D\tilde{w}_{xx}(x, t) - a\tilde{w}_x(x, t) - (g + \lambda)\tilde{w}(x, t) \\ &\quad + \dot{l}(t) (Q(x, l(t)) - P(x, l(t))) \tilde{w}(l(t), t), \end{aligned} \quad (33)$$

$$\tilde{w}_x(0, t) = \gamma_1 \tilde{w}(0, t), \quad (34)$$

$$\tilde{w}(l(t), t) = H^T \tilde{X}(t), \quad (35)$$

$$\dot{\tilde{X}}(t) = (A - LC) \tilde{X}(t), \quad (36)$$

where  $Q(x, y) \in \mathbb{R}$  is also the gain kernel obtained from direct backstepping transformation. Let the ODE observer gain  $L$  be described as  $L = [l_1 \ l_2]^\top$ . To make  $A - LC$  Hurwitz, one can show the conditions for the gains as

$$l_1 > \frac{\tilde{a}l_2}{r_g}, \quad l_2 > \tilde{a}. \quad (37)$$

Taking the time and spatial derivatives of (32) together with the solution of (33)-(35) and the stability of  $\tilde{X}(t)$ , we obtain (23)-(25), and by choosing  $P(x, y) = \tilde{P}(x, y)e^{\frac{\lambda}{2D}(x+y)}$ , (23)-(25) become

$$\tilde{P}_{yy}(x, y) - \tilde{P}_{xx}(x, y) = \frac{\lambda}{2D}\tilde{P}(x, y), \quad (38)$$

$$\tilde{P}(x, x) = e^{-\frac{ax}{2D}} \left( \frac{\lambda}{2D}x + \gamma_1 \right), \quad (39)$$

$$\tilde{P}_x(0, y) = \frac{a}{2D}\tilde{P}(0, y), \quad (40)$$

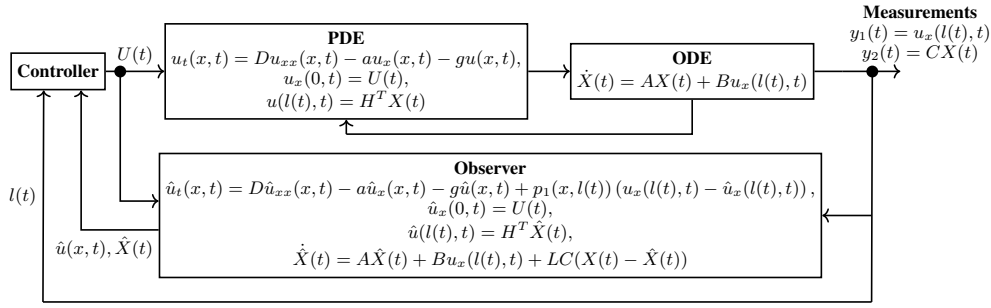


Fig. 3: Block diagram of observer design and output-feedback system

which cannot yield an analytical solution. To guarantee the well-posedness of the solution, we apply the method of successive approximation, by which a numerical solution can be obtained.

### B. Kernel PDE analysis by successive approximations

The method of successive approximation is applied to prove that (38)-(40) is well-posed, which leads to an integral equation for obtaining the solution. First, we apply the following change of spatial coordinate  $\bar{x} = y$ ,  $\bar{y} = x$ , and  $P^*(\bar{x}, \bar{y}) = \tilde{P}(x, y)$ . Then, we have

$$P_{\bar{x}\bar{x}}^*(\bar{x}, \bar{y}) - P_{\bar{y}\bar{y}}^*(\bar{x}, \bar{y}) = \frac{\lambda}{2D} P^*(\bar{x}, \bar{y}), \quad (41)$$

$$P^*(\bar{x}, \bar{x}) = e^{-\frac{\alpha\bar{x}}{2D}} \left( \frac{\lambda}{2D} \bar{x} + \gamma_1 \right), \quad (42)$$

$$P_{\bar{y}}^*(\bar{x}, 0) = \frac{a}{2D} P^*(\bar{x}, 0). \quad (43)$$

To convert gain kernel PDE to integral equation, we introduce

$$\xi = \bar{x} + \bar{y}, \quad \eta = \bar{x} - \bar{y}, \quad P^*(\bar{x}, \bar{y}) = G(\xi, \eta), \quad (44)$$

where  $(\xi, \eta) \in \mathcal{T}_1$  defined as  $\mathcal{T}_1 = \{\xi, \eta : 0 < \xi < 2l(t), 0 < \eta < \min(\xi, 2l(t) - \xi)\}$ . By (44), the conditions (41)–(43) are rewritten with respect to  $G$  as

$$G_{\xi\eta}(\xi, \eta) = \frac{\lambda}{8D} G(\xi, \eta), \quad (45)$$

$$G(\xi, 0) = e^{-\frac{\alpha\xi}{4D}} \left( \frac{\lambda}{4D} \xi + \gamma_1 \right), \quad (46)$$

$$G_{\xi}(\xi, \xi) - G_{\eta}(\xi, \xi) = \frac{a}{2D} G(\xi, \xi). \quad (47)$$

By applying the method of successive approximation, the solution to (45)–(47) is supposed to be in the form of  $G(\xi, \eta) = G_0(\xi, \eta) + F[G](\xi, \eta)$ , where each component is

$$G_0(\xi, \eta) = \frac{\lambda}{2D} e^{-\frac{\alpha}{2D}\eta} \int_0^\eta f(\tau) d\tau + \frac{\lambda}{4D} \int_\eta^\xi e^{-\frac{\alpha}{2D}\tau} f(\tau) d\tau \quad (48)$$

$$F[G](\xi, \eta) = \frac{\lambda}{4D} \int_0^\eta e^{\frac{\alpha}{2D}(\tau-\eta)} \int_0^\tau G(\tau, s) ds d\tau + \frac{\lambda}{8D} \int_\eta^\xi \int_0^\eta G(\tau, s) ds d\tau. \quad (49)$$

where  $f(x) = \left( \left(1 - \frac{\alpha x}{2D}\right) - \frac{2a}{\lambda} \gamma_1 \right)$ . By using the definition of  $G_0$ , we let  $G_{n+1} = F[G_n]$  and because of the positivity of  $a$ ,  $\gamma_1$ ,  $D$ , and  $\lambda$ , we get  $\sup_{x \in [0, l(t)]} f(x) \leq 1$ . Then, the bound of (48) can be obtained as

$$|G_0(\xi, \eta)| \leq \frac{\lambda}{2} \left( \frac{1}{a} + \frac{\bar{l}}{D} \right) =: M. \quad (50)$$

Then, one can obtain

$$|G_{n+1}(\xi, \eta)| \leq M^{n+2} \frac{(\xi + \eta)^{n+1}}{(n+1)!}. \quad (51)$$

Thus,  $G(\xi, \eta) = \sum_{n=0}^{\infty} G_n(\xi, \eta)$ , which converges in  $\mathcal{T}_1$  uniformly, and absolutely. In addition, it is continuous and twice differentiable. Thus,  $G$  has a bound

$$|G(\xi, \eta)| \leq M e^{M(\xi+\eta)}. \quad (52)$$

By following the procedure described in [23], we get  $G(\xi, \eta)$  is unique. Then, we can conclude the following result

$$|P(x, y)| \leq M e^{2Mx}, \quad (53)$$

which guarantees the boundedness of the solution to the gain kernel PDE in (23)–(25).

### C. Direct backstepping transformation

We use the following direct backstepping transformation

$$\tilde{w}(x, t) = \tilde{u}(x, t) - \int_x^{l(t)} Q(x, y) \tilde{u}(y, t) dy. \quad (54)$$

By applying (54) to the observer error system (28)–(31) and the target system (33)–(36), the conditions for the kernel function are obtained as

$$DQ_{xx}(x, y) - aQ_x(x, y) - DQ_{yy}(x, y) - aQ_y(x, y) = \lambda Q(x, y), \quad (55)$$

$$Q(x, x) = -\frac{\lambda}{2D} x + \gamma_1, \quad (56)$$

$$Q_x(0, y) = 0. \quad (57)$$

To make sure the well-posedness of the solution to the kernel PDE above, we apply the following transformation

$Q(x, y) = 2e^{\frac{a}{2D}(x-y)}\tilde{Q}(x, y)$ . Then, the conditions (55)–(57) can be rewritten as

$$\tilde{Q}_{xx}(x, y) - \tilde{Q}_{yy}(x, y) = \frac{\lambda}{D}\tilde{Q}(x, y), \quad (58)$$

$$\tilde{Q}(x, x) = -\frac{\lambda}{4D}x + \frac{\gamma_1}{2}, \quad (59)$$

$$\tilde{Q}_x(0, y) = \frac{a}{D}\tilde{Q}(0, y). \quad (60)$$

This kernel PDE is well-posed, so the solution of  $Q(x, y)$  exists, which means direct transformation exists. As it is in the case of the inverse transformation, the closed-form solution of the direct kernel equation cannot be obtained. By applying the procedure in the previous section, we have the bound as  $|Q(x, y)| \leq Me^{2Mx}$ .

#### D. Stability analysis of observer error system

We consider the following Lyapunov function for the observer error target system

$$\tilde{V} = \tilde{V}_{11} + \tilde{V}_{12} + d_2\tilde{V}_2 + \frac{\gamma_1}{2}\tilde{w}(0, t)^2, \quad (61)$$

where

$$\tilde{V}_{11} = \frac{1}{2}d_1\|\tilde{w}\|^2 := \frac{1}{2}d_1 \int_0^{l(t)} \tilde{w}(x, t)^2 dx, \quad (62)$$

$$\tilde{V}_{12} = \frac{1}{2}\|\tilde{w}_x\|^2 := \frac{1}{2} \int_0^{l(t)} \tilde{w}_x(x, t)^2 dx, \quad (63)$$

$$\tilde{V}_2 = \tilde{X}(t)^\top P \tilde{X}(t), \quad (64)$$

and  $P > 0$  is a positive definite matrix satisfying the Lyapunov equation:

$$(A - LC)^\top P + P(A - LC) = -Q, \quad (65)$$

for some positive definite matrix  $Q$ . Since  $(A - LC)$  is Hurwitz, positive definite matrices  $P$  and  $Q$  exist. In addition, we can denote that  $F(x, \tilde{X}(t)) = \left(P(x, \tilde{X}(t) + l_s) - Q(x, \tilde{X}(t) + l_s)\right) H^\top \tilde{X}(t)$ . Then, we state the following lemma.

**Lemma 1.** Assume that (16) and (17) are satisfied for

$$\bar{v} = \min \left\{ \frac{D}{8l}, \frac{g + \lambda}{2\gamma_1} \right\}, \quad (66)$$

for all time  $t \geq 0$ . Then, we conclude that for sufficiently large enough  $d_1 > 0$  and  $d_2 > 0$ , there exists a positive constant  $\alpha_1 = \min \left\{ d_1 \frac{D}{2}, d_1(D + 2\lambda), (g + 2\lambda), \frac{\lambda_{\min}(Q)}{2\lambda_{\max}(P)} \right\}$  which satisfies the following norm estimates

$$\dot{\tilde{V}} \leq -\alpha_1 \tilde{V}. \quad (67)$$

*Proof.* Taking the time derivative of the Lyapunov functions along the target system (33)–(36), we have

$$\begin{aligned} \dot{\tilde{V}}_{11} &= d_1 D \tilde{w}(l(t), t) \tilde{w}_x(l(t), t) - d_1 \left( D\gamma_1 - \frac{a}{2} \right) \tilde{w}(0, t)^2 \\ &\quad - d_1 \dot{l}(t) \int_0^{l(t)} \tilde{w}(x, t) F(x, \tilde{X}(t)) dx - a \frac{d_1}{2} \tilde{w}(l(t), t)^2 \\ &\quad - d_1 D \|\tilde{w}_x\|^2 - d_1 (g + \lambda) \|\tilde{w}\|^2 + d_1 \frac{\dot{l}(t)}{2} \tilde{w}(l(t), t)^2 \end{aligned} \quad (68)$$

$$\begin{aligned} \dot{\tilde{V}}_{12} &= H^\top (A - LC) \tilde{X}(t) \tilde{w}_x(l(t), t) - \frac{1}{2} \dot{l}(t) \tilde{w}_x(l(t), t)^2 \\ &\quad - \tilde{w}_x(0, t) \tilde{w}_t(0, t) - D \|\tilde{w}_{xx}\|^2 \\ &\quad + \int_0^{l(t)} a \tilde{w}_{xx} \tilde{w}_x dx - (g + \lambda) \|\tilde{w}_x\|^2 \\ &\quad + (g + \lambda) \tilde{w}(l(t), t) \tilde{w}_x(l(t), t) - (g + \lambda) \gamma_1 \tilde{w}(0, t)^2 \\ &\quad - \dot{l}(t) \int_0^{l(t)} \tilde{w}_{xx}(x, t) F(x, \tilde{X}(t)) dx, \end{aligned} \quad (69)$$

$$\dot{\tilde{V}}_2 = -\tilde{X}(t)^\top Q \tilde{X}(t), \quad (70)$$

where  $d_1 > 0$ . Applying Young's inequality and (36), and by using (35) to the time derivative of  $\tilde{V}_{11}$  in (68) leads to

$$\begin{aligned} \dot{\tilde{V}}_{11} &\leq -d_1 \left( D\gamma_1 - \frac{a}{2} \right) \tilde{w}(0, t)^2 - d_1 D \|\tilde{w}_x\|^2 \\ &\quad - d_1 (g + \lambda) \|\tilde{w}\|^2 + \frac{D\epsilon_1}{2} \tilde{w}_x(l(t), t)^2 \\ &\quad - d_1 \dot{l}(t) \int_0^{l(t)} \tilde{w}(x, t) F(x, \tilde{X}(t)) dx \\ &\quad + \left( d_1^2 \frac{D}{2\epsilon_1} + d_1 \frac{\dot{l}(t)}{2} - d_1 \frac{a}{2} \right) \tilde{w}(l(t), t)^2, \end{aligned} \quad (71)$$

where  $\epsilon_1 > 0$  is an arbitrarily small constant. Similarly, using Agmon's inequalities and Young's inequality (defined in [8]) into the time derivative of  $\tilde{V}_{12}$  in (69) gives us

$$\begin{aligned} \dot{\tilde{V}}_{12} &\leq \gamma_1^2 \left( D\epsilon_1 + \epsilon_2 + \epsilon_3(g + \lambda) + \bar{v} + \frac{\bar{v}\epsilon_5}{2} \right) \tilde{w}(0, t)^2 \\ &\quad - \left( \gamma_1(g + \lambda) \right) \tilde{w}(0, t)^2 - \left( D - \frac{D}{4} \right) \|\tilde{w}_{xx}\|^2 \\ &\quad - \left( -2\bar{l}(D\epsilon_1 + \epsilon_2 + \epsilon_3(g + \lambda) + \epsilon_4\bar{v} + \bar{v}) \right) \|\tilde{w}_{xx}\|^2 \\ &\quad - \left( (g + \lambda) - \frac{a^2}{D} \right) \|\tilde{w}_x\|^2 - \gamma_1 \tilde{w}(0, t) \tilde{w}_t(0, t) \\ &\quad + \left( \left( d_1^2 \frac{D}{2\epsilon_1} + d_1 \frac{a}{2} + d_1 \frac{\bar{v}}{2} + \frac{(g + \lambda)}{2\epsilon_3} \right) \lambda_{\max}(HH^\top) \right. \\ &\quad \left. + \frac{1}{2\epsilon_2} \lambda_{\max}((H^\top(A - LC))^2) \right) \tilde{X}^\top \tilde{X} \\ &\quad + \frac{|\dot{l}(t)|}{2\epsilon_4} F(l(t), \tilde{X}(t))^2 + \frac{|\dot{l}(t)|}{2\epsilon_5} \gamma_1 F(0, \tilde{X}(t))^2 \\ &\quad + |\dot{l}(t)| \int_0^{l(t)} \tilde{w}_x(x, t) F_x(x, \tilde{X}(t)) dx, \end{aligned} \quad (72)$$

where  $\epsilon_i > 0$  for  $i = \{1, \dots, 5\}$  are arbitrarily small constants. The time derivative of  $\tilde{V}_2$  in (70) is given by

$$\dot{\tilde{V}}_2 \leq -\lambda_{\min}(Q) \tilde{X}^\top \tilde{X}. \quad (73)$$

Then, we use Young's and Cauchy-Schwarz Inequalities for  $F(\cdot, \cdot)$  terms. There exists positive constants  $L_i > 0$ , for  $i = 1, 2, 3, 4$ , we have  $F(0, \tilde{X}(t))^2 \leq L_1 \tilde{X}^\top \tilde{X}$ ,  $F(l(t), \tilde{X}(t))^2 \leq L_2 \tilde{X}^\top \tilde{X}$ ,  $\int_0^{l(t)} F(x, \tilde{X}(t))^2 dx \leq L_3 \tilde{X}^\top \tilde{X}$ , and  $\int_0^{l(t)} F_x(x, \tilde{X}(t))^2 dx \leq L_4 \tilde{X}^\top \tilde{X}$ . With these

inequalities and (71)-(73), (72) becomes

$$\begin{aligned}
\dot{V} \leq & -\frac{D}{2} \|\tilde{w}_{xx}\|^2 - d_1 \frac{D\gamma_1}{2} \tilde{w}(0,t)^2 - d_1(g+\lambda) \|\tilde{w}\|^2 \\
& + \frac{\bar{v}\epsilon_6}{2} \|\tilde{w}\|^2 - \left( d_1 D + (g+\lambda) - \frac{a^2}{D} - \frac{\bar{v}\epsilon_7}{2} \right) \|\tilde{w}_x\|^2 \\
& - \gamma_1 \tilde{w}(0,t) \tilde{w}_t(0,t) + d_1 \frac{\bar{v}}{2} L_1 |\tilde{X}(t)|^2 + \frac{\bar{v}}{2\epsilon_4} L_2 \bar{v}^2 \\
& + d_1^2 \frac{\bar{v}}{2\epsilon_6} L_3 \bar{v}^2 + \frac{\bar{v}}{2\epsilon_7} L_4 |\tilde{X}(t)|^2 - d_2 \lambda_{\min}(Q) |\tilde{X}(t)|^2 \\
& + \left( \left( d_1^2 \frac{D}{2\epsilon_1} + d_1 \frac{a}{2} + d_1 \frac{\bar{v}}{2} + \frac{(g+\lambda)}{2\epsilon_3} \right) \lambda_{\max}(HH^\top) \right. \\
& \left. + \frac{1}{2\epsilon_2} \lambda_{\max}((H^\top(A-LC))^2) \right) |\tilde{X}(t)|^2. \quad (74)
\end{aligned}$$

By using positive definiteness, we recall

$$\lambda_{\min}(P) X^\top X \leq X^\top P X \leq \lambda_{\max}(P) X^\top X, \quad (75)$$

where  $\lambda_{\min}(P) > 0$  and  $\lambda_{\max}(P) > 0$  are the smallest and the largest eigenvalues of  $P$ . Finally, by recalling  $\gamma_1 \geq \frac{D}{a}$ , we can choose constants  $d_1$  and  $d_2$  as

$$\begin{aligned}
d_1 \geq & \frac{2a^2 + D\bar{v}\epsilon_7}{D^2}, \quad (76) \\
d_2 \geq & \frac{2}{\lambda_{\min}(Q)} \left( \left( \frac{D}{2\epsilon_1} + d_1 \frac{a+\bar{v}}{2} \right) \lambda_{\max}(HH^\top) \right. \\
& + \frac{(g+\lambda)}{2\epsilon_3} \lambda_{\max}(HH^\top) + \frac{\lambda_{\max}((H^\top(A-LC))^2)}{2\epsilon_2} \\
& \left. + \left( \frac{d_1}{2} L_1 + \frac{1}{2\epsilon_4} L_2 + \frac{d_1^2}{2\epsilon_6} L_3 + \frac{1}{2\epsilon_7} L_4 \right) \bar{v} \right). \quad (77)
\end{aligned}$$

Thus, one can show that (74) leads to

$$\begin{aligned}
\dot{V} \leq & -d_1 \frac{D\gamma_1}{2} \tilde{w}(0,t)^2 - d_1(D+2\lambda) \tilde{V}_{12} - (g+2\lambda) \tilde{V}_{11} \\
& - d_2 \frac{\lambda_{\min}(Q)}{2\lambda_{\max}(P)} \tilde{V}_2 \\
\leq & -\alpha_1 \tilde{V}. \quad (78)
\end{aligned}$$

Thus, Lemma 1 holds.  $\square$

Hence, the target  $\tilde{w}$ -system (33)-(36) is exponentially stable at the origin. Because of the invertibility of backstepping transformation, the stability of  $\tilde{w}$ -system promotes to the original  $\tilde{u}$ -system (28)-(31) exponentially stable. This completes the proof of Theorem 1.

#### IV. OBSERVER-BASED OUTPUT-FEEDBACK CONTROL

In this section, an output-feedback control law is constructed using the observer designed in Section III with the measurements (18), and the following theorem holds.

**Theorem 2.** Consider the closed-loop system (10)-(13) with the measurements (18), and the observer (19)-(22) under the output-feedback control law:

$$\begin{aligned}
U(t) = & \frac{D\gamma_2 - \beta}{D} \hat{u}(0,t) + \phi'(-l(t))^\top - \gamma_2 \phi(-l(t))^\top \hat{X}(t) \\
& - \frac{1}{D} \int_0^{l(t)} (\phi'(-y)^\top - \gamma_2 \phi(-y)^\top) B \hat{u}(y,t) dy \quad (79)
\end{aligned}$$

where  $\gamma_2 \geq \frac{a}{D}$  and  $\phi(x)$  is

$$\phi(x)^\top = [H^\top \quad K^\top - \frac{1}{D} H^\top B H^\top] e^{N_1 x} \begin{bmatrix} I \\ 0 \end{bmatrix}. \quad (80)$$

The matrices  $K = [k_1 \quad k_2]$  and  $N_1 \in \mathbb{R}^{4 \times 4}$  is defined as

$$N_1 = \begin{bmatrix} 0 & \frac{1}{D} (gI + A + \frac{a}{D} B H^\top) \\ I & \frac{1}{D} (B H^\top + aI) \end{bmatrix}, \quad (81)$$

where  $k_1 > \frac{\bar{a}}{\beta}$ , and  $k_2 > 0$ . Then, there exist positive constants  $\bar{M} > 0$ ,  $\kappa > 0$  and  $\zeta > 0$  such that if  $\Phi(0) < \bar{M}$  where  $\Phi(t) := \|u\|_{\mathcal{H}_1}^2 + |X|^2 + \|\hat{u}\|_{\mathcal{H}_1}^2 + |\hat{X}|^2$ , then the following norm estimate holds:

$$\Phi(t) \leq \zeta \Phi(0) \exp(-\kappa t). \quad (82)$$

Namely, the closed-loop system is locally stable in the sense of  $\mathcal{H}_1$ -norm.

##### A. Backstepping transformation

The following transformation from  $(\hat{u}, \hat{X})$  into  $(\hat{w}, \hat{X})$  is implemented by using the gain kernels proposed in [8]

$$\begin{aligned}
\hat{w}(x,t) = & \hat{u}(x,t) - \int_x^{l(t)} k(x,y) \hat{u}(y,t) dy \\
& - \phi(x-l(t))^\top \hat{X}(t), \quad (83)
\end{aligned}$$

and the reverse transformation is

$$\begin{aligned}
\hat{u}(x,t) = & \hat{w}(x,t) + \int_x^{l(t)} q(x,y) \hat{w}(y,t) dy \\
& + \varphi(x-l(t))^\top \hat{X}(t). \quad (84)
\end{aligned}$$

Taking the time and spatial derivatives of the transformation above, the target  $\hat{w}$ -system is obtained as

$$\begin{aligned}
\hat{w}_t = & D \hat{w}_{xx} - a \hat{w}_x - g \hat{w} + \dot{l}(t) E(x, \hat{X}(t)) \\
& + p_1(x, l(t)) \tilde{u}_x(l(t), t) \\
& - \int_x^{l(t)} k(x,y) p_1(y, l(t)) \tilde{u}_x(l(t), t) dy, \quad (85)
\end{aligned}$$

$$\hat{w}_x(0,t) = \gamma_2 \hat{w}(0,t), \quad (86)$$

$$\hat{w}(l(t), t) = 0, \quad (87)$$

$$\begin{aligned}
\dot{\hat{X}}(t) = & (A + BK) \hat{X}(t) + B \hat{w}_x(l(t), t) \\
& + B \tilde{u}_x(l(t), t) + LC \tilde{X}(t), \quad (88)
\end{aligned}$$

where we denote  $E(x, \hat{X}(t)) = (\phi'(x - \hat{X}(t) - l_s)^\top - k(x, \hat{X}(t) + l_s) H^\top) \hat{X}(t)$ . By evaluating the spatial derivative of (83) at  $x = 0$ , we derive the control law as in (79).

The gain kernels  $k(x,y)$  and  $\phi(x)$  are derived in [8].

##### B. Stability analysis

Define the Lyapunov function for closed-loop system as

$$V_{\text{tot}} = c_1 \tilde{V}(t) + \hat{V}_{11} + \hat{V}_{12} + \frac{1}{2} \gamma_2 \hat{w}(0,t)^2 + d_4 \hat{V}_2 \quad (89)$$

where  $c_1 > 0$  is chosen to sufficiently large,  $\tilde{V}(t)$  is defined in (61)–(64) and each term in  $\hat{V}(t)$  is

$$\hat{V}_{11}(t) = \frac{1}{2}d_3\|\hat{w}\|^2 := \frac{1}{2}d_3 \int_0^{l(t)} \hat{w}(x,t)^2 dx, \quad (90)$$

$$\hat{V}_{12}(t) = \frac{1}{2}\|\hat{w}_x\|^2 := \frac{1}{2} \int_0^{l(t)} \hat{w}_x(x,t)^2 dx, \quad (91)$$

$$\hat{V}_2(t) = \hat{X}(t)^\top \hat{P} \hat{X}(t). \quad (92)$$

Lyapunov function of closed-loop system is also written as

$$\begin{aligned} V_{\text{tot}}(t) = & c_1 \frac{1}{2} (d_1 \|\tilde{w}\|^2 + \|\tilde{w}_x\|^2) + \frac{1}{2} (d_3 \|\hat{w}\|^2 + \|\hat{w}_x\|^2) \\ & + c_1 d_2 \tilde{X}(t)^\top P \tilde{X}(t) + d_4 \hat{X}(t)^\top \hat{P} \hat{X}(t) \\ & + \frac{1}{2} (c_1 \gamma_1 \tilde{w}(0,t)^2 + \gamma_2 \hat{w}(0,t)^2). \end{aligned} \quad (93)$$

Then, we state the following lemma.

**Lemma 2.** *Let Assumptions 1 and 2 hold with*

$$\bar{v} \leq \min \left\{ \frac{g}{3\gamma_2}, \frac{D}{8\bar{l}}, \frac{g+\lambda}{2\gamma_1} \right\}, \quad (94)$$

for all time  $t \geq 0$ . Then, for sufficiently large enough  $d_3 > 0$  and  $d_4 > 0$ , there exists a positive constant  $\alpha > 0$  and  $\beta > 0$  such that the following norm estimates holds

$$\dot{V}_{\text{tot}} \leq -\alpha V_{\text{tot}} + \beta V_{\text{tot}}^{3/2}. \quad (95)$$

*Proof.* By applying Young's, Cauchy-Schwarz, Poincaré's, and Agmon's inequalities, with the help of Assumption 1 and 2, and following the same strategy that is offered in the [8] for the Lyapunov analysis, one can derive

$$\dot{V}_{\text{tot}} \leq -\alpha V_{\text{tot}} + \beta V_{\text{tot}}^{3/2}, \quad (96)$$

for

$$\alpha = \min \left\{ \frac{1}{2}\alpha_1, d_3 \frac{D}{2}, \frac{g}{2}, d_4 \frac{\lambda_{\min}(\hat{Q})}{4\lambda_{\max}(\hat{P})} \right\}, \quad (97)$$

$$\beta = \frac{r_g e_1^\top}{\lambda_{\min}(\hat{P})} \left( \frac{1}{2}L_5 + \frac{1}{2}L_6 + d_3 \frac{1}{2\varepsilon_3}L_7 + \frac{1}{2}L_8 \right), \quad (98)$$

where  $\varepsilon_3 \leq \frac{g}{\bar{v}}$  such that Lemma 2 holds.  $\square$

To prove local stability, Lemma 2 from [8] guarantees to the convergence in all time. It satisfies that  $V_{\text{tot}}(t) < M_1$  holds for some  $M > 0$ , then  $|\tilde{X}| < r$ . Lemma 3 from [8] proves that for (96), if  $V_{\text{tot}}(0) < M$ , then  $V_{\text{tot}}(t) < M$  for all  $t > 0$ . In addition,  $\dot{l}(t)$  can be written as  $\dot{l}(t) = r_g e_1^\top X(t)$ , so we can bound  $\dot{l}(t)$  to handle in the norm equivalence as

$$|\dot{l}(t)| \leq r_g e_1^\top \left( \sqrt{\frac{\tilde{V}_2}{\lambda_{\min}(P)}} + \sqrt{\frac{\hat{V}_2}{\lambda_{\min}(\hat{P})}} \right) \quad (99)$$

This leads us  $|\dot{l}(t)|^2 \leq \delta^2 V_{\text{tot}}(t)$ . Thus,

$$V_{\text{tot}}(t) \leq V_{\text{tot}}(0) \exp\left(-\frac{\alpha}{2}t\right). \quad (100)$$

The norm equivalence between the target and original systems is shown using the direct and inverse transformations of both observer target and observer error target systems. Taking

TABLE I: Biological constants and control parameters

Parameter	Value	Parameter	Value
$D$	$10 \times 10^{-6} m^2/s$	$\tilde{r}_g$	0.053
$a$	$1 \times 10^{-8} m/s$	$\gamma$	$10^4$
$g$	$5 \times 10^{-7} s^{-1}$	$l_c$	$4\mu m$
$r_g$	$1.783 \times 10^{-5} m^4/(mol \cdot s)$	$l_s$	$12\mu m$
$c_\infty$	0.0119 mol/m <sup>3</sup>	$l_0$	$1\mu m$

square of (32), (54), (83), and (84) and applying Young's and Cauchy-Schwarz inequalities, and integrating on  $[0, l(t)]$ , one can get the norm inequalities for the target system ( $\hat{w}, \hat{w}_x, \tilde{w}, \tilde{w}_x$ ). Then, let  $\Psi = \|\hat{w}\|_{H_1}^2 + |\hat{X}|^2 + \|\tilde{w}\|_{H_1}^2 + |\tilde{X}|^2$ . Using the norm inequalities for each term in  $\Psi$  and (93), one can obtain  $\underline{M} > 0$  and  $\underline{M} < 0$  such that

$$\underline{M}\Psi(t) \leq V_{\text{tot}}(t) \leq \overline{M}\Psi(t) \quad (101)$$

holds. Therefore, we get

$$\Psi(t) \leq \frac{\overline{M}}{\underline{M}} \exp\left(-\frac{\alpha}{2}t\right) \Psi(0) \quad (102)$$

Now, we apply the norm equivalence argument to the transformations between the target system and the original system by using  $u(x,t) = \tilde{u}(x,t) + \hat{u}(x,t)$  and  $X(t) = \tilde{X}(t) + \hat{X}(t)$ . Let  $\Phi(t) = \|u\|_{H_1}^2 + |X|^2 + \|\tilde{u}\|_{H_1}^2 + |\tilde{X}|^2$  so, one can obtain  $\underline{N} > 0$ , and  $\underline{N} < 0$  such that

$$\underline{N}\Phi(t) \leq \Psi(t) \leq \overline{N}\Phi(t) \quad (103)$$

Therefore, we get

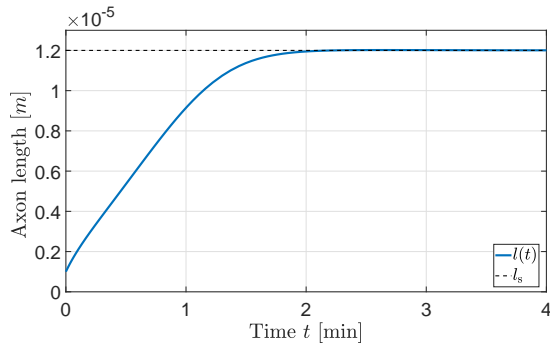
$$\Phi(t) \leq \frac{\overline{N}}{\underline{N}} \exp\left(-\frac{\alpha}{2}t\right) \Phi(0) \quad (104)$$

Namely, since the backstepping transformation for the target error system and for the observer system are invertible, the local stability of  $(\tilde{w}, \tilde{X}, \hat{w}, \hat{X})$  guarantees the local stability of  $(u, X, \hat{u}, \hat{X})$ , which completes the proof of Theorem 2.

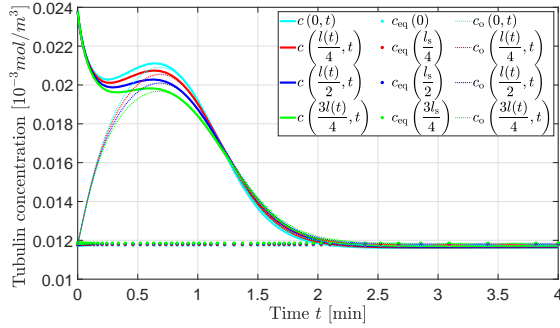
## V. NUMERICAL SIMULATION

Numerical simulation is performed for the plant (10)–(13), and observer (19)–(22) with a designed control law (79). We use the biological constants proposed in [10], as shown in Table I. The initial conditions for the plant is set as  $c_0(x) = 2c_\infty$  for tubulin concentration along the axon, and  $l_0 = 1\mu m$  for the axon length. In addition, initial conditions for the observer are chosen  $c_o(x,0) = 0$  for all along the axon where the subscript o denotes the observer. The control and observer gains for ODE parts of the closed-loop system are  $k_1 = -0.1$ ,  $k_2 = 10^{13}$ ,  $l_1 = 1$ , and  $l_2 = 0.1$ . The gain parameter,  $\lambda$ , is chosen 0.05 to obtain fast convergence.

Fig. 4a shows that the axon length converges to the desired axon length  $l_s$ . Fig. 4b illustrates that the observer states converge to the actual tubulin concentration, by which the estimation of the tubulin concentration along the axon is successfully achieved. In addition, the tubulin concentration along the axon converges to the steady-state solution, which demonstrates the effectiveness of the proposed output-feedback control law.



(a) The axon length converges to the desired length.



(b) The estimated tubulin concentration,  $c_o(x, t) = \hat{u}(x, t) + c_{eq}(x)$ , generated by the observer in (19)–(22) and shown in Fig. 3, converges all along the axon to the actual, unmeasured concentration  $c(x, t)$  by about  $t = 0.75$  min. Thereafter, both  $c_o$  and  $c$  converge together to the steady-state  $c_{eq}(x)$  from  $t = 0.75$  min till about  $t = 2$  min. Note that  $c_o$  converges to  $c$  faster than  $c$  converges to  $c_{eq}$  and faster than  $l$  converges to  $l_s$ .

Fig. 4: Closed-loop output-feedback response.

## VI. CONCLUSIONS

This study proposes a novel output-feedback control for a coupled PDE-ODE dynamics with a moving boundary for neuron growth model by applying the PDE backstepping technique. We proposed a PDE-observer with designing an observer gain via backstepping, with showing the stability analysis to estimate the unknown states in the plant dynamics. Then, we designed the output-feedback controller for the axon elongation problem to achieve the desired length of the axon. Next, the stability analysis of the closed-loop system under the proposed output-feedback controller is provided. Finally, we have verified our theoretical results in the simulation results using the biological parameters.

For further research, it is also feasible to establish the local stability without applying linearization with the output-feedback control law. Further studies about the relation between ECM and tubulin production would make it the controller applicable in clinical trials such as ChABC.

## REFERENCES

[1] C. S. Barros, S. J. Franco, and U. Müller, “Extracellular matrix: functions in the nervous system,” *Cold Spring Harbor perspectives in biology*, vol. 3, no. 1, p. a005108, 2011.  
[2] E. J. Bradbury and L. M. Carter, “Manipulating the glial scar: chondroitinase abc as a therapy for spinal cord injury,” *Brain research bulletin*, vol. 84, no. 4-5, pp. 306–316, 2011.

[3] M. Buisson-Fenet, S. Koga, and M. Krstic, “Control of piston position in inviscid gas by bilateral boundary actuation,” in *2018 IEEE Conference on Decision and Control (CDC)*. IEEE, 2018, pp. 5622–5627.  
[4] E. Burnside and E. Bradbury, “Manipulating the extracellular matrix and its role in brain and spinal cord plasticity and repair,” *Neuropathology and applied neurobiology*, vol. 40, no. 1, pp. 26–59, 2014.  
[5] R. Buxbaum and S. Heidemann, “A thermodynamic model for force integration and microtubule assembly during axonal elongation,” *Journal of theoretical biology*, vol. 134, no. 3, pp. 379–390, 1988.  
[6] J.-M. Coron, R. Vazquez, M. Krstic, and G. Bastin, “Local exponential  $h^2$  stabilization of a  $2 \times 2$  quasilinear hyperbolic system using backstepping,” *SIAM Journal on Control and Optimization*, vol. 51, no. 3, pp. 2005–2035, 2013.  
[7] W. Dauer and S. Przedborski, “Parkinson’s disease: mechanisms and models,” *Neuron*, vol. 39, no. 6, pp. 889–909, 2003.  
[8] C. Demir, S. Koga, and M. Krstic, “Neuron growth control by pde backstepping: Axon length regulation by tubulin flux actuation in soma,” *arXiv preprint arXiv:2109.14095*, 2021.  
[9] S. Diehl, E. Henningsson, A. Heyden, and S. Perna, “A one-dimensional moving-boundary model for tubulin-driven axonal growth,” *Journal of Theoretical Biology*, vol. 358, pp. 194–207, 2014.  
[10] —, “A one-dimensional moving-boundary model for tubulin-driven axonal growth,” *Journal of theoretical biology*, vol. 358, pp. 194–207, 2014.  
[11] C. Frantz, K. M. Stewart, and V. M. Weaver, “The extracellular matrix at a glance,” *Journal of cell science*, vol. 123, no. 24, pp. 4195–4200, 2010.  
[12] E. M. Izhikevich, *Dynamical systems in neuroscience*. MIT press, 2007.  
[13] J.-P. Julien, “Neurofilament functions in health and disease,” *Current opinion in neurobiology*, vol. 9, no. 5, pp. 554–560, 1999.  
[14] S. Karimi-Abdolrezaee, E. Eftekharpour, J. Wang, D. Schut, and M. G. Fehlings, “Synergistic effects of transplanted adult neural stem/progenitor cells, chondroitinase, and growth factors promote functional repair and plasticity of the chronically injured spinal cord,” *Journal of Neuroscience*, vol. 30, no. 5, pp. 1657–1676, 2010.  
[15] S. Koga, M. Diagne, and M. Krstic, “Control and state estimation of the one-phase stefan problem via backstepping design,” *IEEE Transactions on Automatic Control*, vol. 64, no. 2, pp. 510–525, 2018.  
[16] S. Koga and M. Krstic, *Materials Phase Change PDE Control and Estimation: From Additive Manufacturing to Polar Ice*. Springer Nature, 2020.  
[17] M. Krstic and A. Smyshlyaev, *Boundary control of PDEs: A course on backstepping designs*. SIAM, 2008.  
[18] X. Z. Liu, X. M. Xu, R. Hu, C. Du, S. X. Zhang, J. W. McDonald, H. X. Dong, Y. J. Wu, G. S. Fan, M. F. Jacquin, *et al.*, “Neuronal and glial apoptosis after traumatic spinal cord injury,” *Journal of Neuroscience*, vol. 17, no. 14, pp. 5395–5406, 1997.  
[19] R. B. Maccioni, J. P. Muñoz, and L. Barbeito, “The molecular bases of alzheimer’s disease and other neurodegenerative disorders,” *Archives of medical research*, vol. 32, no. 5, pp. 367–381, 2001.  
[20] D. R. McLean and B. P. Graham, “Stability in a mathematical model of neurite elongation,” *Mathematical medicine and biology: a journal of the IMA*, vol. 23, no. 2, pp. 101–117, 2006.  
[21] D. R. McLean, A. van Ooyen, and B. P. Graham, “Continuum model for tubulin-driven neurite elongation,” *Neurocomputing*, vol. 58, pp. 511–516, 2004.  
[22] L. Ribar and R. Sepulchre, “Neuromorphic control,” *arXiv preprint arXiv:2011.04441*, 2020.  
[23] A. Smyshlyaev and M. Krstic, “Closed-form boundary state feedbacks for a class of 1-d partial integro-differential equations,” *IEEE Transactions on Automatic Control*, vol. 49, no. 12, pp. 2185–2202, 2004.  
[24] L. Squire, D. Berg, F. E. Bloom, S. Du Lac, A. Ghosh, and N. C. Spitzer, *Fundamental neuroscience*. Academic press, 2012.  
[25] G. A. Susto and M. Krstic, “Control of pde-ode cascades with neumann interconnections,” *Journal of the Franklin Institute*, vol. 347, no. 1, pp. 284–314, 2010.  
[26] S. Tang and C. Xie, “State and output feedback boundary control for a coupled pde-ode system,” *Systems & Control Letters*, vol. 60, no. 8, pp. 540–545, 2011.  
[27] M. P. Van Veen and J. Van Pelt, “Neuritic growth rate described by modeling microtubule dynamics,” *Bulletin of mathematical biology*, vol. 56, no. 2, pp. 249–273, 1994.